Hypoxia mimetic induces lipid accumulation through mitochondrial dysfunction and stimulates autophagy in murine preadipocyte cell line

Ana Patrícia Marques, Joana Rosmaninho-Salgado, Marta Estrada, Vera Cortez, Rui Jorge Nobre, Cláudia Cavadas

PII: S0304-4165(16)30489-5
DOI: doi: 10.1016/j.bbagen.2016.12.005
Reference: BBAGEN 28704

To appear in: *BBA - General Subjects*

Received date: 22 August 2016
Revised date: 29 November 2016
Accepted date: 5 December 2016

Please cite this article as: Ana Patrícia Marques, Joana Rosmaninho-Salgado, Marta Estrada, Vera Cortez, Rui Jorge Nobre, Cláudia Cavadas, Hypoxia mimetic induces lipid accumulation through mitochondrial dysfunction and stimulates autophagy in murine preadipocyte cell line, *BBA - General Subjects* (2016), doi: 10.1016/j.bbagen.2016.12.005

Title: Hypoxia mimetic induces lipid accumulation through mitochondrial dysfunction and stimulates autophagy in murine preadipocyte cell line

Authors: Ana Patrícia Marques[a,b,*] , Joana Rosmaninho-Salgado[a,c,*], Marta Estrada[a], Vera Cortez[a], Rui Jorge Nobre[a], Cláudia Cavadas[a,d]

[a]CNC - Center for Neuroscience and Cell Biology, University of Coimbra, 3004-504 Coimbra, Portugal

[b]PDBEB – Doctoral Program in Experimental Biology and Biomedicine, Interdisciplinary Research Institute (III-UC), University of Coimbra, 3004-504 Coimbra, Portugal

[c]Department of Medical Genetics, Pediatric Unit, Coimbra Hospital and Universitary Center (CHUC), 3000-602 Coimbra, Portugal

[d]Faculty of Pharmacy, University of Coimbra, 3000-548 Coimbra, Portugal

[*] These authors contributed equally to this work.

Corresponding author: Cláudia Cavadas

Address: Center for Neuroscience and Cell Biology

Rua Larga

University of Coimbra

3004-517 Coimbra, Portugal

Email: ccavadas@uc.pt

Abstract

Background: Hypoxia occurs within adipose tissue of obese human and mice. However, its role in adipose tissue regulation is still controversial.

Methods: We used murine preadipocyte 3T3-L1 cells and hypoxia was induced by using hypoxia mimetic agents, as $CoCl_2$. To study adipocyte differentiation, we evaluated the adipocyte markers (PPARγ, C/EBPα and aP2), and a preadipocyte marker (Pref-1) by qPCR, western blotting and immunofluorescence. Lipid accumulation was evaluated by Oil red-O assay and by analyzing perilipin levels by western blotting and immunofluorescence. The effect of $CoCl_2$ in microRNAs, miR-27a and miR-27b, levels was evaluated by qPCR. We also assessed the mitochondrial membrane potential, reactive oxygen species (ROS), superoxide and ATP production. The effect of hypoxia mimetic in autophagy was determined by LC3B and p62 levels evaluation by western blotting.

Results: Our results show that the hypoxia mimetic cobalt chloride increases lipid accumulation with no expression of PPARγ2. Furthermore, using qPCR we observed that the hypoxia mimetic increases microRNAs miR-27a and miR-27b, which are known to block PPARγ2 expression. In contrast, cobalt chloride induces mitochondrial dysfunction, and increases ROS production and autophagy. Moreover, an antioxidant agent, glutathione, prevents lipid accumulation induced by hypoxia mimetic indicating that ROS are responsible for hypoxia-induced lipid accumulation.

Conclusions: All these results taken together suggest that hypoxia mimetic blocks differentiation and induces autophagy. Hypoxia mimetic also induces lipid accumulation through mitochondrial dysfunction and ROS accumulation.

General Significance: This study highlights the importance of adipocyte response to hypoxia, which might impair adipocyte metabolism and compromise adipose tissue function.

Key words: hypoxia, adipogenesis, mitochondrial dysfunction, reactive oxygen species, autophagy

1. Introduction

Obesity is characterized by an excessive increase of white adipose tissue, which is associated with an oxygenation reduction of adipose tissue in mice and humans [1-4]. Adipocytes become hypertrophic during the development of obesity, becoming larger than the diffusion distance limit of oxygen [5, 6]. Therefore, oxygen is not able to reach the cells causing local hypoxia in expanding adipocytes. Cellular response to hypoxia is manifested by the activation of the hypoxia-inducible factor-1 (HIF-1), a heterodimeric transcription factor that is considered a molecular oxygen sensor [7]. HIF-1 mediates the cellular response to hypoxia, regulating several target genes that encode for proteins involved in angiogenesis, cell proliferation, apoptosis and energy metabolism [8]. It is clear that hypoxia is an important condition that regulates white adipose tissue homeostasis, being a major contributor for adipose tissue dysfunction in obesity.

The formation of adipose tissue is dependent on preadipocyte differentiation to adipocytes, which are mature cells specialized in lipid accumulation. This differentiation process is called adipogenesis and it is driven by the coordinated expression of various transcription factors, such as the peroxisome proliferator-activated receptor 2 (PPARγ2), CCAAT/enhancer binding protein α (C/EBPα) and adipocyte Protein 2 (aP2) [9]. Given the importance of oxygen levels for energy homeostasis and cell differentiation, hypoxic condition regulates adipocyte differentiation [10, 11]. The effect of hypoxic status on lipid accumulation is controversial, since there are conflicting reports, which describe hypoxia as both increasing and decreasing cytoplasmic lipid accumulation [10, 12-14]. It has been demonstrated that hypoxia inhibits adipogenesis

through decreasing PPARγ2 expression [10, 11]. In addition, HIF-1α suppresses fatty acid β-oxidation and this mechanism is responsible for adipose tissue expansion attenuation [15]. Furthermore, most of the studies about the role of hypoxia on adipocytes describe its effect either on lipid accumulation or on PPARγ expression. However, hypoxia may also lead to changes in other intracellular pathways, in particular mitochondrial dysfunction, production of reactive oxygen species (ROS), and also the formation of microRNAs (miRs), which can modify differentiation and lipid accumulation within adipocytes. As adipogenesis occurs, adipocytes store lipids in the form of triglycerides in lipid droplets, which are considered a marker of differentiated adipocytes. However, it was described that lipid accumulation can occur in adipocyte and non-adipocyte cell models independently of differentiation status and PPARγ and as a consequence of mitochondrial dysfunction [16, 17] or apoptosis [18]. Moreover, it has been reported that microRNAs modulate adipocyte differentiation [19, 20]. The miR-143 induces preadipocyte 3T3-L1 differentiation and the miR-130 is involved in the blockage of PPARγ expression [19-21]. In addition, miR-27a and miR-27b levels are higher in adipose tissue of obese *ob/ob* mice than in lean animals [22]. However, it was also described that miR-27a was down-regulated in mature adipocytes of high-fat diet-fed obese mice comparing to normal chow diet-fed lean mice [23]. Although there are some works about the effect of miRs on adipocyte differentiation, the effect of hypoxia on miRs regulation in adipose tissue is not well known.

Autophagy is known to be necessary to normal adipocyte differentiation [24]. Moreover, it is known that hypoxia can induce autophagy in other non-adipose cells [25, 26], few works report the

effect of autophagy in adipose tissue [24]. Using either the 3T3-L1 cell line or mouse embryonic fibroblasts, normal adipogenesis is associated with increased autophagic activity [24, 27], but it is described that autophagy is increased in the adipose tissue of obese individuals [28].

The aim of this work is to evaluate the role of hypoxia mimetic, cobalt chloride, on the normal physiology of adipocytes, by determining lipid accumulation, PPARγ2 expression, miRNA expression, mitochondrial changes and autophagy. We hypothesized that lipid accumulation in adipocytes, induced by hypoxia mimetic, is due to mitochondrial dysfunction and that hypoxia induces autophagy.

2. Materials and Methods

2.1. Cell culture

3T3-L1, a murine preadipocyte cell line (American type Culture Collection – LGC Promochem) was plated in 22.1 cm^2 flasks and was maintained in high glucose (4.5 g/L D-glucose) Dulbecco's Modified Eagle Medium (DMEM-HG; Sigma) with phenol red, supplemented with 10% (vol/vol) heat-inactivated fetal bovine serum, 100 U/mL penicillin, 100 µg/mL streptomycin, 2.5 mM l-glutamine and 1.5 g/L $NaHCO_3$ at 37 °C and 5% CO_2/air.

2.2. Cell Differentiation protocol

Preadipocytes were plated in 24-well plates (25000 cells/well) until they reached confluence (day 0). After 2 days, the medium was removed and replaced by DMEM-HG supplemented with a cell differentiation cocktail: 3-isobutyl-1-methylxanthine (IBMX, 0.5 mM) and dexamethasone (0.25 µM) (day 2) (Sigma). After 3 days (day 5),

the culture medium was changed to DMEM-HG without the differentiation cocktail. Every 2 days, the medium was renewed until day 9.

2.3. Experimental Conditions

For the positive control, it was used insulin (1 µg/mL) (Sigma). To evaluate the effect of hypoxia on adipogenesis, 3T3-L1 preadipocytes were treated with $CoCl_2$ (100 µM) or deferoxamine mesylate (DFO) (100 µM) (Sigma), hypoxia mimetic agents. Mitochondrial complex I inhibitor, rotenone (1 µM) or Glutathione (GSH) (50 µM) (Sigma) were added to the medium (without insulin) to evaluate their effect on adipocytes differentiation.

2.4. Lipid accumulation quantification by Oil red-O staining

Seven days after induction of preadipocyte differentiation, cells were washed twice with phosphate buffered saline (PBS) and fixed with p-formaldehyde (4% in PBS) for 30 minutes at room temperature. Cells were then washed twice with PBS, once with distilled water, and stained with Oil Red-O dye (6:4, 0.6% Oil red-O dye in water) (Sigma) for one hour before being washed three times with water. Finally, Oil red-O staining was dissolved in 200 µL of isopropanol, and the absorbance measured at 500 nm.

2.5. Oil Red-O fluorescent staining

Prior to the permeabilization step of immunofluorescence protocol, cells were washed twice with PBS and fixed with p-formaldehyde (4% in PBS) for 30 minutes at room temperature. Cells were then washed twice with PBS and stained with Oil Red-O dye (6:4, 0.6%

Oil red-O dye in water) for one hour before being washed three times with PBS.

2.6. Immunofluorescence

Following fixation with p-formaldehyde (4% in PBS) and permeabilization with Triton-X100 (1% in PBS), nonspecific binding was blocked with 3% bovine serum albumin (BSA) and 0.2% Tween20 in PBS. Cells were incubated overnight at 4 ºC with the following primary antibodies, rabbit anti-PPARγ (1:500; Santa Cruz Biotechnology), rabbit anti-perilipin A (1:100; Cell Signalling), mouse anti-pref-1 (1:500; Abcam), or mouse anti-HIF-1α (1:1000; Abcam). After rinsing with PBS, the cells were incubated with the appropriate secondary antibody (Molecular Probes, Invitrogen) for 1 hour (1:200), at room temperature. All antibodies were prepared in blocking solution (PBS containing 3% of BSA). Nuclei were labeled with Hoechst 33342 (1 µg/ml) (Molecular Probes, Invitrogen) for 3 minutes, after incubation with the secondary antibody and coverslips were mounted on glass slides. Cells were visualized using a fluorescence microscope (Carl Zeiss Axio Observer Z1) and the images were acquired with the Carl Zeiss Zen software or the laser scanning microscope LSM 510 META (Zeiss, Jena, Germany).

2.7. Mitotracker and Mitosox

For direct labeling of mitochondria, cells were stained with 500 nM MitoTracker Red CMXRos (Molecular Probes, Invitrogen) for 30 minutes, and fixed with p-formaldehyde (4% in PBS). Alternatively, for detection of superoxide in the mitochondria of live cells, cells were stained with 5 µM MitoSOX (Molecular Probes, Invitrogen) for 10 minutes at 37 ºC. Cells were counterstained with

Hoechst 33342 (1 µg/ml) for 3 minutes. Coverslips were mounted on glass slides, the cells were visualized using a fluorescence microscope (Carl Zeiss Axio Observer Z1) and the images were acquired with the Carl Zeiss Zen software or in a laser scanning microscope LSM 510 META (Zeiss, Jena, Germany).

2.8. Western blotting

Western blotting was performed as described in the Supplementary Methods.

2.9. Quantitative real-time PCR

Total RNA extraction, reverse transcription, and quantitative real-time PCR (qPCR) analysis was performed as described in the Supplementary Methods.

2.10. Lactate measurements

Lactate was measured in cell supernatants using a Lactate Colorimetric Assay Kit (Abcam), according to the manufacturer's protocol. Data were normalized in terms of protein concentration determined by the Bradford assay (Biorad).

2.11. Determination of ATP content

Cells were disrupted with lysis buffer on ice. Extracts were centrifuged at 13000 x g for 10 minutes at 4 °C and supernatants were collected. ATP was measured using the ATP Bioluminescence assay kit CLS II (Roche Diagnostics GmbH, 1699 695, Mannheim, Germany), according to the manufacturer's protocol. Light emission was recorded for 30 seconds by a photon counting luminometer.

Relative ATP level was normalized in terms of protein concentration determined by the Bradford assay (Biorad).

2.12. Reactive Oxygen Species (ROS) measurements

Cells were washed twice with PBS, and incubated with a cell-permeant indicator for reactive oxygen species (5 µM H_2DCFDA, Invitrogen) in PBS for 30 minutes at 37 °C. The fluorescent signal was read at excitation of 492 nm and emission of 517 nm in a microplate reader. ROS levels were normalized in terms of protein concentration determined by the Bradford assay (Biorad).

2.13. Cell proliferation assay

Proliferation of 3T3-L1 preadipocytes was determined using the resazurin reduction assay. Preadipocytes were plated in 48-well plates (100000 cells/well) in DMEM medium with 10% FBS. Twenty-four hours after cell plating, cells were serum-deprived during twelve hours and then $CoCl_2$ treatment was done in triplicates in a serum free DMEM. After 24h of $CoCl_2$ incubations, cells were incubated with resazurin and the absorbance was read at 570 and 600 nm. To quantify cell proliferation the ratio between 570/600 nm was done, and all results were compared to control and expressed as percentage of control.

2.14. TUNEL assay

Cells were fixed, permeabilized, washed twice, incubated for 1 hour at 37 °C with the TUNEL mix (*in situ* cell death kit; Roche Applied Science) and washed again. Cells were counterstained with Hoechst 33342 (1 µg/mL) for 3 minutes. For the positive control, fixed and permeabilized cells were treated with DNase I recombinant.

Coverslips were mounted on glass slides, the cells were visualized using a fluorescence microscope Zeiss PALM Microscope.

2.15. Statistical analysis

Results are expressed as mean ± standard error of the mean (SEM). Data were analyzed using one-way analysis of variance (ANOVA) followed by Dunnet's or Bonferroni's post-hoc test, or t-test, as indicated in figure legends. A value of $p<0.05$ was considered significant. Prism 6.0 (GraphPad Software, San Diego, CA) was used for all statistical analysis.

3. Results

3.1. Hypoxia mimetic agent $CoCl_2$ induces lipid accumulation without PPARγ2 expression

Adaptation to low oxygen is mediated by the transcription factor HIF-1α [7]. Hypoxia stabilizes HIF-1α, which induces the expression of several genes [7, 8]. Hypoxia (1% O_2), cobalt chloride ($CoCl_2$) and deferoxamine (DFO) can stabilize HIF-1α through inhibition of HIF-1α hydroxylation by prolyl and arginyl hydroxylases [29, 30]. Therefore, $CoCl_2$ and DFO are widely used as a hypoxia mimetics [29, 30]. We used both $CoCl_2$ and DFO, as hypoxia mimetic, to evaluate the impact of hypoxia on preadipocyte differentiation. As expected, we observed that $CoCl_2$ and DFO (100 μM) increases HIF-1α immunoreactivity in the nucleus of 3T3-L1 preadipocytes (Figure S1). The effect of hypoxia mimetic in adipocyte differentiation was evaluated by measuring PPARγ, C/EBPα and aP2, transcription factors critical in differentiation process and also lipid accumulation, characteristic of mature adipocytes. $CoCl_2$ decreases PPARγ, C/EBPα and aP2 mRNA levels, compared to

control (Fig.1A-C). By western blotting, we observed that the adipogenic marker PPARγ2 is present in adipocytes incubated with insulin (1 µg/mL) but it is not detected when preadipocytes are submitted to hypoxic mimetic conditions (Fig. 1D). As expected, insulin-treated preadipocytes differentiated into adipocytes as shown by the two well-known adipogenic markers: increase of cytoplasmic lipid droplets coupled with PPARγ staining in the nucleus (Fig. 1E). Hypoxic mimetic conditions ($CoCl_2$) increases cytoplasmic lipid droplet accumulation but no nuclear PPARγ staining was observed (Fig. 1E). Moreover, these lipid droplets are smaller, more numerous, and have a diffuse pattern compared to lipid droplets in adipocytes under control conditions (Fig. 1F). Lipid accumulation was measured by Oil red-O staining and hypoxia increases lipid accumulation by 63.2 ± 10.5%, compared to control (Fig.1G). We also treated cells with another hypoxia mimetic (DFO) and evaluated lipid accumulation and PPARγ expression. We observed that DFO treatment also inhibited PPARγ2 levels and increased lipid accumulation (Fig. 1D and 1G).

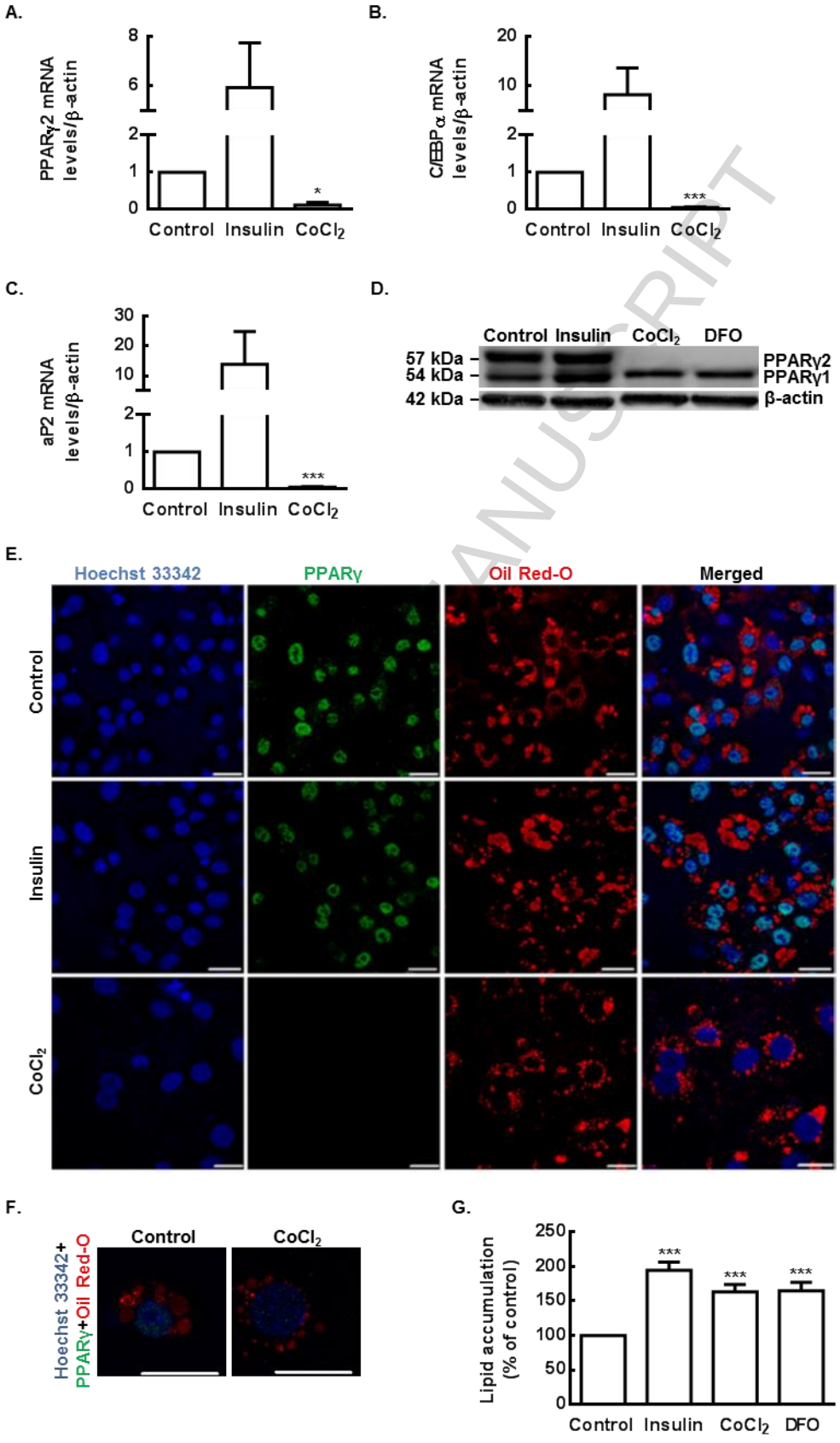

Figure 1 – Hypoxia mimetic inhibits PPARγ2, C/EBPα and aP2 expression but increases lipid accumulation. 3T3-L1

preadipocytes were induced to differentiate and were treated with insulin (1 µg/mL), cobalt chloride ($CoCl_2$ 100 µM) or deferoxamine (DFO 100 µM) for seven days. **(A-C)** qPCR to determine the expression of PPARγ2**,** C/EBPα and aP2 mRNA. n=3 * $p<0.05$, *** $p<0.001$, significantly different from control group. One-way ANOVA was used as statistical test. (D) Representative image of western blotting for PPARγ and β-actin (loading control). (E and F) Representative images of immunofluorescence for PPARγ (green) performed after Oil red-O that stains the lipid droplets (red). Nuclei were stained with Hoescht 33342 (blue). Scale bar: 20 µm. (G) Oil red-O staining to quantify lipid accumulation. n=9 *** $p<0.001$, significantly different from control group. One-way ANOVA was used as statistical test.

Because hypoxia mimetic induces lipid accumulation without differentiation we investigated perilipin expression, which is an adipocyte-specific protein that coats lipid droplets. Adipocytes differentiated with insulin (1 µg/mL) showed an increase in perilipin expression, while in hypoxic mimetic conditions perilipin is not detected (Fig. 2A and B). Since lipid droplets are present in these adipocytes with no PPARγ and perilipin expression, we decided to evaluate whether preadipocytes under hypoxia mimetic condition were arrested in the preadipocyte state. And to do that, we evaluated a preadipocyte marker preadipocyte factor 1 (pref-1) [31]. As expected, we observed, by western blotting and immunofluorescence, that insulin decreases pref-1 immunoreactivity (Fig. 2C and D). Also, hypoxia mimetic condition inhibits pref-1 expression (Fig. 2C and 2D), suggesting that hypoxia mimetic does not arrest preadipocytes in an undifferentiated state.

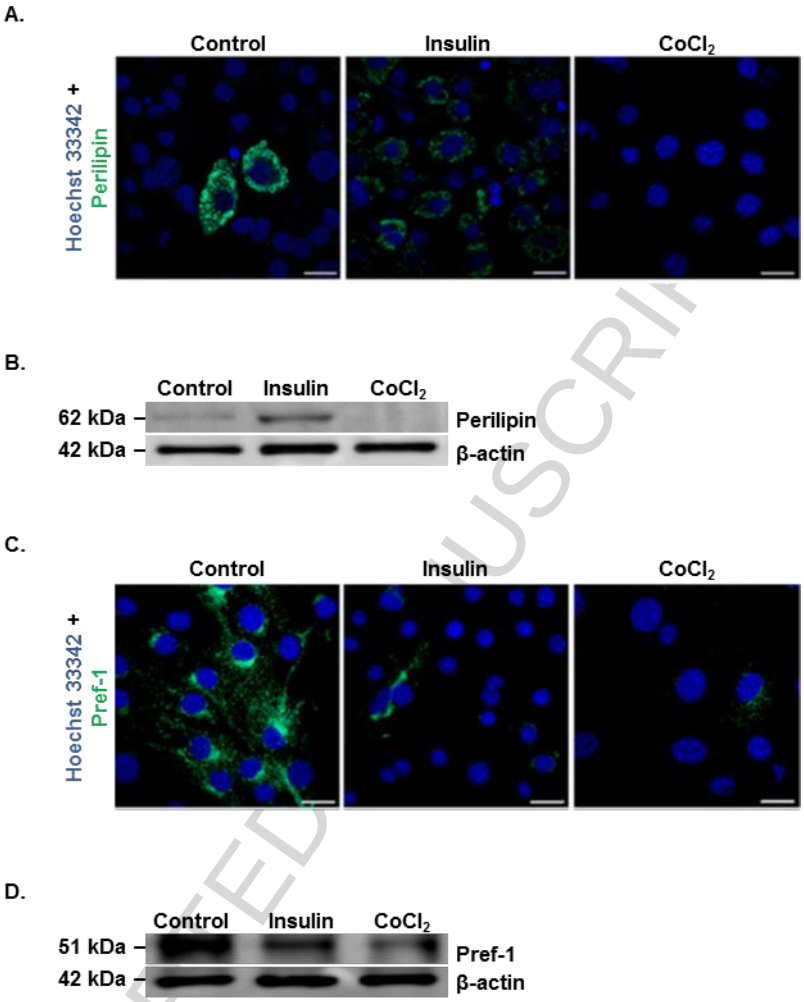

Figure 2 – Hypoxia mimetic inhibits perilipin and pref-1 protein levels. 3T3-L1 preadipocytes were induced to differentiate and were treated with insulin (1 µg/ml) or cobalt chloride ($CoCl_2$ 100 µM) for seven days. (A and C) Representative images of immunofluorescence for (A) perilipin (green) or (C) pref-1 (green). Nuclei were stained with Hoescht 33342 (blue). Scale bar: 20 µm (B and D) Representative image of western blotting for (B) perilipin or (D) pref-1 and β-actin (loading control).

Since it was also described that increased lipid droplet formation occurs during cell death [32], we investigated the effect of hypoxia mimetic $CoCl_2$ in cell proliferation by using resazurin reduction assay and apoptosis by TUNEL assay and evaluation of p53 levels by

western blotting. Our results showed an increase of 22.7 ± 12.3 % on preadipocyte proliferation when incubated for 24h with $CoCl_2$ (Fig. S2A). However, $CoCl_2$-treated cells showed no alterations in p53 levels and TUNEL-positive cells (Fig. S2B-C).

3.2. Adipocyte differentiation is blocked by miR-27a and miR-27b induction

It has been reported that miR-27a and miR-27b are downregulated during adipogenesis and that their overexpression impairs adipocyte differentiation by inhibiting PPARγ expression [22, 23, 33]. We hypothesized that hypoxia mimetic inhibits adipocyte differentiation by miR-27a and miR-27b increase which in turn inhibit PPARγ2 expression. To test whether inhibition of PPARγ2 expression by the hypoxia mimetic $CoCl_2$ is modulated by miR-27a and miR-27b expression, we measured the levels of miR-27a and miR-27b under hypoxic mimetic conditions. As can be seen in Figure 3, both microRNAs are increased when cells were treated with $CoCl_2$: 3.4 ± 0.3 and 4.5 ± 0.6-fold increase for miR-27a and miR-27b expression, respectively (Fig. 3). These results show that hypoxia increases miR-27a and miR-27b, which probably will impair adipocyte differentiation.

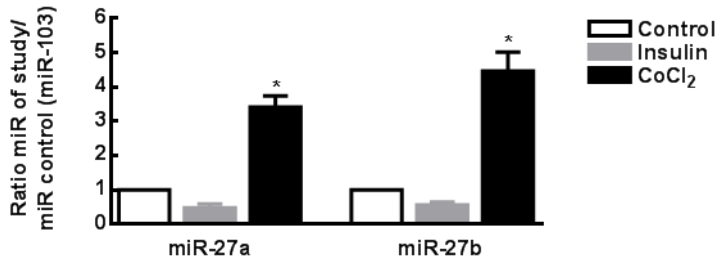

Figure 3 – Hypoxia mimetic increases mir-27a and mir-27b expression. 3T3-L1 preadipocytes were induced to differentiate and were treated with insulin (1 µg/ml) or cobalt chloride ($CoCl_2$ 100 µM)

for seven days. qPCR for miR-27a and miR-27b was performed. The control miR was considered the miR-103. Results are expressed as the ratio miR-27a/miR-103 or miR-27b/miR-103 levels. n=3 * $p<0.05$ compared to control. One-way ANOVA was used as statistical test.

3.3. Mitochondrial dysfunction and ROS are responsible for lipid accumulation induced by hypoxia mimetic

Hypoxia may induce other cellular dysfunctions in preadipocytes, such as mitochondrial dysfunction [34]. In agreement, we observed that hypoxic mimetic condition decreases the number of normal and energized mitochondria and induces a disrupted mitochondrial network with fewer interconnections (Fig. 4A). We also observed that hypoxic mimetic condition increases the lactate production by 40.7 ± 5.3% (Fig. 4C), decreases the cellular content of ATP by 66.5 ± 4.0% (Fig. 4D) and also increases 110.2 ± 7.9% the production of ROS, compared to control (Fig. 4E).

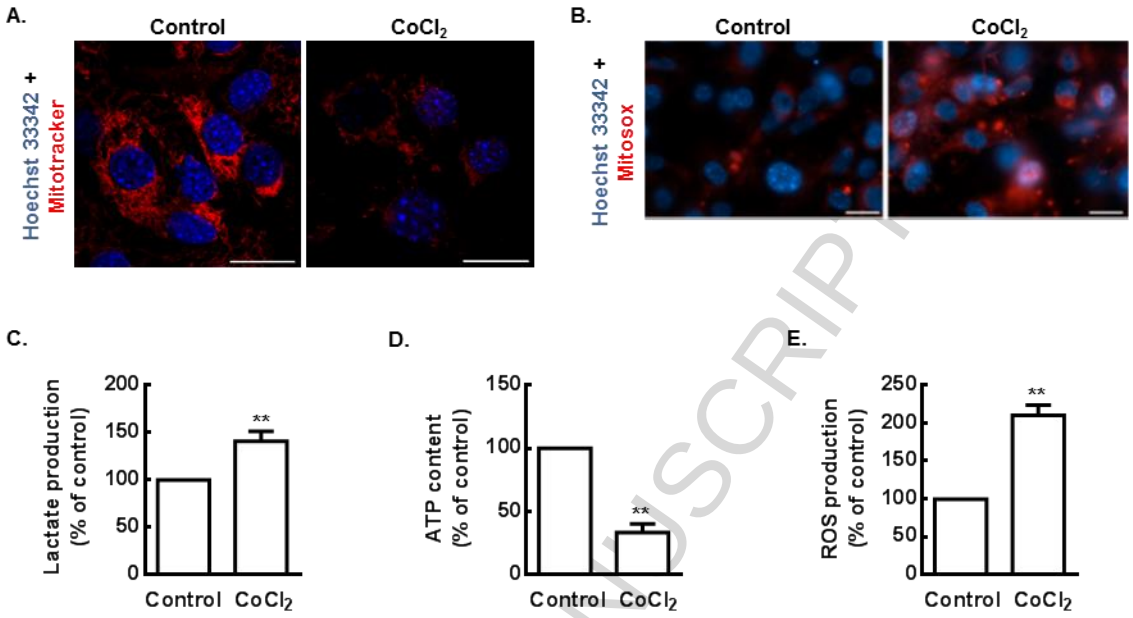

Figure 4 – Hypoxia mimetic induces mitochondrial dysfunction. 3T3-L1 preadipocytes were induced to differentiate and were treated with cobalt chloride ($CoCl_2$ 100 μM) for seven days. (A) Mitochondrial network was evaluated by using MitoTracker Red CMXRos stained (red). (B) Mitochondrial superoxide production was evaluated by using MitoSOX Red (red). Nuclei were stained with Hoescht 33342 (blue). A representative image is shown in this figure. Scale bar: 20 μm (C) Lactate production was quantified. (D) Intracellular ATP was evaluated. (E) Reactive oxygen species (ROS) production was evaluated. Values were normalized by amount of protein. n=3-4 ** $p<0.01$ compared to control. t-test was used as statistical test.

To relate mitochondrial dysfunction with adipogenesis, cells were treated with an inhibitor of mitochondrial complex I, rotenone (1 μM). As also seen in hypoxic mimetic conditions, rotenone increases lipid accumulation by 48.4 ± 7.2%, compared to control, without the adipocyte differentiation markers, PPARγ2 and perilipin (Fig. 5).

Taken together, these results suggest that mitochondrial inhibition caused by hypoxia mimetic condition is contributing to lipid accumulation increase.

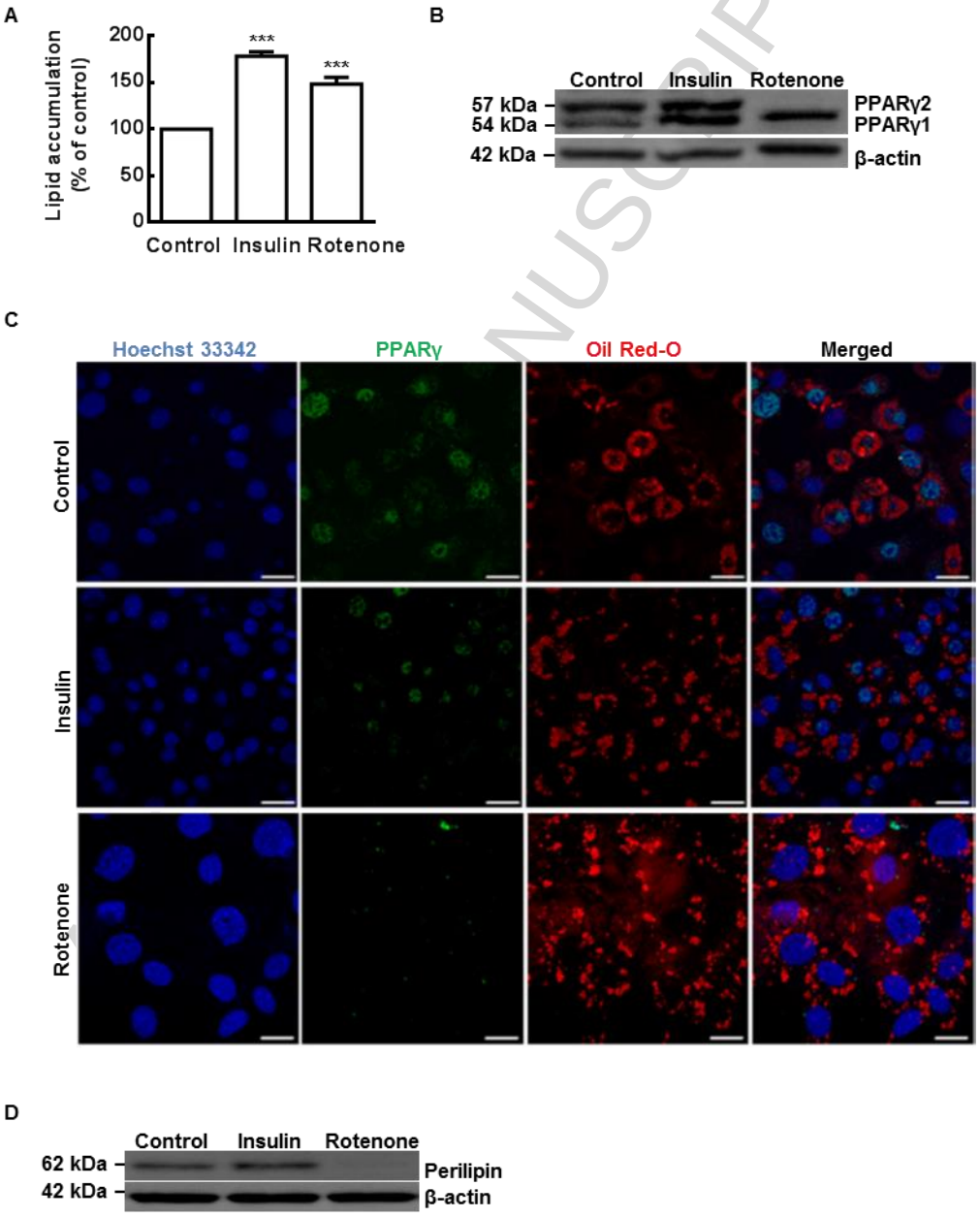

Figure 5 – Mitochondrial dysfunction is involved on lipid accumulation and PPARγ inhibition induced by hypoxia mimetic. 3T3-L1 preadipocytes were induced to differentiate and were treated with insulin (1 µg/ml) or rotenone (1 µM) for seven days. (A) Oil red-O staining to quantify lipid accumulation. n=8 ***

$p<0.001$, significantly different from control group. One-way ANOVA was used as statistical test. (B) Representative image of western blotting for PPARγ and β-actin (loading control). (C) Representative images of immunofluorescence for PPARγ (green) performed after Oil red-O that stains the lipid droplets (red). Nuclei were stained with Hoescht 33342 (blue). Scale bar: 20 μm (D) Representative image of western blotting for perilipin and β-actin (loading control).

In order to investigate whether ROS production was due to mitochondrial dysfunction, we evaluated the production of superoxide by mitochondria using MitoSOX Red. MitoSOX Red selectively targets mitochondria, being oxidized by superoxide but not by other reactive oxygen species and reactive nitrogen species. We observed that $CoCl_2$ increases superoxide production by mitochondria when compared to control (Fig. 4B). This provides direct evidence that $CoCl_2$-induced ROS production is derived from mitochondria. To further study the contribution of ROS on lipid accumulation induced by hypoxia mimetic, we treated cells with $CoCl_2$ in the presence or absence of glutathione which is an antioxidant, reducing ROS availability. We observed that glutathione prevents 37.8 ± 3.2% lipid accumulation induced by $CoCl_2$ (Fig. 6). This result suggests that ROS production is responsible for lipid accumulation induced by hypoxia mimetic.

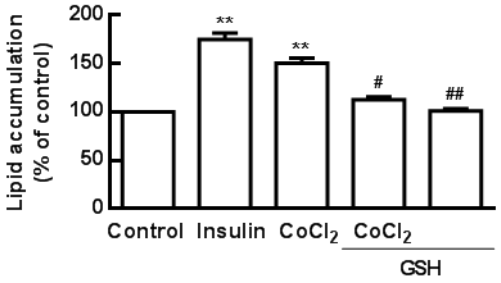

Figure 6 – Reactive oxygen species are responsible for lipid accumulation that occurs in 3T3-L1 preadipocyte hypoxia mimetic-treatment. 3T3-L1 preadipocytes were induced to differentiate and were treated with cobalt chloride ($CoCl_2$ 100 μM) in the presence or absence of glutathione (GSH 50 μM) for seven days. (A) Oil red-O staining to quantify lipid accumulation. n=4 ** $p<0.01$, significantly different from control group; # $p<0.05$, ## $p<0.01$, significantly different from $CoCl_2$. One-way ANOVA was used as statistical test.

3.4. Hypoxia mimetic induces autophagy

Autophagy is a physiological protective mechanism that is also described to occur as a consequence of cell stress. Autophagy can be induced in response to a hypoxic condition [25, 26]. Moreover, ROS have also been shown to mediate autophagy induction [35]. To investigate whether hypoxia regulates autophagy in 3T3-L1 preadipocyte cell line, we measured the protein levels of the transient autophagosomal membrane-bound form of LC3B (LC3B-II) and p62 or sequestosome 1 (SQSTM1), widely used as markers for monitoring the autophagic process [36]. Hypoxia mimetic ($CoCl_2$) decreases LC3B-II levels by 65.7 ± 10.2% (Fig. 7A) and also decreases p62 levels by 49.8 ± 6.0% (Fig. 7B), when compared to

control. These results suggest an increase of autophagic clearance in this hypoxia mimetic condition.

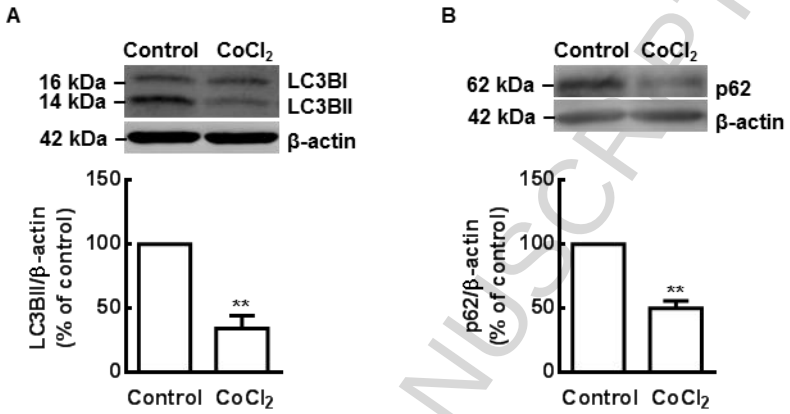

Figure 7 – Hypoxia mimetic-treatment induces autophagy. 3T3-L1 preadipocytes were induced to differentiate and were treated with cobalt chloride ($CoCl_2$ 100 µM) for seven days. Whole-cell extracts were assayed for (A) LC3B or (B) p62 and β-actin (loading control) immunoreactivity by western blotting. Mean ± SEM, n=4-6 ** $p<0.01$ compared to control. t-test was used as statistical test.

4. Discussion

The present work shows that the hypoxia mimetic, $CoCl_2$ (100 µM) induces lipid accumulation without PPARγ2, perilipin or the preadipocyte marker, pref-1 expression. In addition, the absence of PPARγ2 expression can be related to an increase of microRNAs miR-27a and miR-27b that have been described to inhibit PPARγ2. Since we observed that $CoCl_2$ induces mitochondrial dysfunction and ROS increase, we suggest that the lipid droplets induced by hypoxia mimetic condition could be a consequence of the mitochondrial dysfunction and, consequently, lead to inhibition or dysfunction of adipocyte differentiation and can be prevented by an

antioxidant agent, glutathione. Furthermore, hypoxia and ROS have been reported as inducers of autophagy [25, 26, 35]. We observed that hypoxia mimetic is also responsible for autophagy induction in these cells.

$CoCl_2$ is widely used as a hypoxia mimetic and is known to induce the accumulation of HIF-1α in cell cultures, by inhibiting prolyl hydroxylases [30]. HIF-1α does not mediate all the effects of hypoxia but it is an important part of this cellular response. The use of $CoCl_2$ allows us to distinguish the hypoxia effect that occurs specifically through HIF-1α.

Most works that studied the effect of hypoxia on adipocyte differentiation described the effect of hypoxia on PPARγ expression or on lipid accumulation, and use very different hypoxic treatment durations [10, 11]. Our results are in agreement with other works that have shown PPARγ2, C/EBPα and aP2 expression inhibition by hypoxia or hypoxia mimetics, suggesting that hypoxia inhibits adipocyte differentiation [10-12, 14, 37, 38]. PPARγ is a master regulator of adipogenesis. Alternative splicing and differential promoter use result in two PPARγ isoforms, a ubiquitously expressed PPARγ1 and PPARγ2 that is primarily expressed in adipocytes. PPARγ1 is the most abundant isoform in preadipocytes, while PPARγ2 is adipocyte-specific. *In vitro* PPARγ2 is more adipogenic than PPARγ1 [39]. Cells treated with insulin showed an increase in PPARγ2 suggesting adipocyte differentiation but $CoCl_2$ prevents adipogenesis as shown by a downregulation of PPARγ2 expression which is not observed in PPARγ1.

However, other studies showed that hypoxia or hypoxic mimetic also inhibits lipid accumulation [10, 11, 14]. Our results are in agreement with a study that shows that $CoCl_2$ induces cytoplasmatic lipid

accumulation in 3T3-L1 preadipocytes [13]. Increased lipid accumulation was also described in bone marrow stromal cells under hypoxic conditions [40]. Another group showed similar results in human bone marrow stromal cells, hMSC-TERT [12], where hypoxia induces an atypical nature of lipid accumulation with no change in marker genes characteristic of mature adipocytes, such as PPARγ2 [12]. The authors suggest that adipogenesis may occur through PPARγ2–dependent and –independent pathways [12]. Moreover, it was described that adipocyte-derived exosomes from hypoxic conditions, which contain lipogenic enzymes, promoted lipid accumulation in non-stressed, normoxic cells [41]. Moreover, we hypothesized that the inhibition of PPARγ2 in hypoxic mimetic conditions most probably occur due to an increase of specific miRNAs. In fact, it has previously been described that some miRNAs regulate adipogenesis: the mir-143 induces differentiation of murine 3T3-L1 and human preadipocytes [20, 21], while miR-27 and miR–130 families inhibit this process [19, 22, 23, 33]. In addition, miR-27a overexpression in 3T3-L1 preadipocytes suppresses PPARγ expression and adipocyte differentiation [22, 23]. Another family member, miR-27b is down-regulated during adipocyte differentiation, and binds to the 3'UTR of PPARγ while repressing PPARγ2 protein levels [33]. miR-27 was also shown to have a role in repressing adipogenic lineage commitment in C3H10T1/2 cells [42]. Interestingly, in mature adipocytes from obese mice lower miR-27a expression was found, compared to mature adipocytes of lean mice, indicating that down-regulation in miR-27a is necessary for adipocyte hypertrophy [23]. On the other hand, it was also described that expression levels of both miR-27a and miR-27b were significantly increased in the adipose tissue from the *ob*/*ob*

mice, as compared with the genetically matched lean mice [22]. In addition, it has also been reported that hypoxia induces a 2-fold and 1.5-fold increase of miR-27a and miR-27b levels, respectively [22]. These results suggest that miR-27 function by inhibiting PPARγ expression and, consequently, preventing adipocytes from entering into the stage of differentiation [22]. From these observations, we evaluated the effect of the hypoxia mimetic $CoCl_2$ on miR-27a and miR-27b expression and observed that the expression of these microRNAs miR-27a and miR-27b increase and may consequently inhibit PPARγ2 expression. These results may explain the fact that preadipocytes treated with $CoCl_2$ have an increase in cytoplasmic lipid droplet accumulation without increasing PPARγ2.

We have further investigated other mechanisms that could explain the lipid droplet accumulation induced by hypoxia mimetic condition. Since some studies have already shown that alterations in mitochondrial function lead to an increase in lipid accumulation [16, 43], we studied the putative role of mitochondrial changes on lipid droplet accumulation induced by hypoxia mimetic. In fact, as with $CoCl_2$, we also observed that, rotenone, an inhibitor of mitochondrial electron transport of complex I, increases lipid droplet accumulation in cytoplasm without nuclear PPARγ2 expression. Furthermore, we also observed that the antioxidant glutathione prevents the lipid accumulation induced by $CoCl_2$. Mitochondrial dysfunction induced by hypoxia mimetic is also strongly supported by the decrease in mitochondrial network, increase in lactate release in the medium, decrease in ATP production and an increased ROS production induced by $CoCl_2$. One of the initial steps in the response of cells to hypoxia is adaptation at the mitochondrial level by reducing the amount of the high O_2-consuming process of oxidative

phosphorylation [6]. As a consequence, there is a switch to anaerobic glycolysis for energy production [6]. A decrease in ATP production and increase in lactate production then occur [6]. The increase of ROS was described to modulate adipocyte differentiation [44, 45]. The high levels of ROS have already been shown in adipocytes isolated from obese mice [46, 47], and also during the differentiation of 3T3-L1 preadipocytes into adipocytes [45]. Others have also shown that mitochondrial dysfunction in adipocytes leads to increased triglycerides storage [16, 43]. Moreover, the glutathione prevention of hypoxia-induced lipid accumulation is in agreement with a study in other cell model, in which the inhibition of mitochondrial oxidative damage induces lipid-β-oxidation recovery accompanied by a decrease on fatty acid incorporation into triglycerides [18].

Autophagy constitutes an important protective mechanism that allows cell to eliminate damaged components to maintain nutrient and energy homeostasis. Moreover, several forms of stress can also activate autophagy. Hypoxia has been described as a stimulus for the induction of autophagy in other cell types [25, 26]. Autophagy has also been described to occur as a consequence of ROS production [35]. Taking this into account we investigated the effect of hypoxia and consequent ROS production in autophagy. In the present study, increased autophagic activity was detected in adipocytes under hypoxia mimetic treatment. To the best of our knowledge, this is the first study to report the effects of hypoxia on autophagy induction in adipocytes. The role of autophagy on adipocytes development and function was studied by others [24, 48]. During adipocyte differentiation of 3T3-L1 cell line or primary mouse embryonic

fibroblasts (MEFs), others observed increased autophagy [24]. Moreover, MEFs derived from atg5 and atg7 knockout mice exhibit drastically reduced adipogenesis efficiency [24, 48]. The knockdown of atg5 and atg7 in 3T3-L1 preadipocytes also decreased the markers of adipocyte differentiation, which was confirmed by studies with pharmacological inhibitors, 3-methyladenine and chloroquine [27]. Newborn Atg5 knockout mice have less subcutaneous adipocytes than wild-type, suggesting that autophagy is important for adipose tissue development [24]. The importance of autophagy in adipogenesis *in vivo* was confirmed in adipocyte-specific Atg7-knockout mice [27, 48]. These mutant mice are leaner, have decreased white adipose tissue mass and have adipocytes with features characteristic of brown adipocytes, smaller, containing multilocular lipid droplets, increased number of mitochondria and increased cytoplasmic volume [27, 48]. Furthermore, in obesity, human adipose tissue and adipocytes show increased autophagy [28]. Functional consequence of increased autophagy in adipose tissue of obese people is not known.

Taking these results together, the present study both extends our understanding of the effect of hypoxia on adipocyte biology and lipid metabolism, providing a possible explanation for hypoxic lipogenesis. It highlights the importance of preadipocyte response to hypoxia which induces autophagy and also induces mitochondrial dysfunction and reactive oxygen species leading to lipid accumulation, which might impair adipocyte metabolism and also compromise its normal function, which can be partially reversed by antioxidant treatment. These conclusions need to be further studied

for its *in vivo* implications and to validate the results with hypoxic conditions (<1% O_2).

Acknowledgments: We thank Célia A. Aveleira and Paulo J. Oliveira for all the useful suggestions and advice. This work was supported by FEDER funds through the Operational Programme Factors Competitiveness - COMPETE 2020 and by National Funds through FCT - Foundation for Science and Technology under the Strategic Project (UID/NEU/04539/2013), PTDC/SAU-FCF/102415/2008, SFRH/BPD/31547/2006, SFRH/BD/51674/2011, SFRH/BPD/78424/2011); also funded by QREN – Projeto Mais Centro – "Aging, Stress And Chronic Diseases: From Mechanisms To Therapeutics" and by a Project Grant for Obesity investigation provided by the Portuguese Society of Endocrinology and Metabolism (SPEDM) and Abbot; L'Oreal Women for Science Program (FCT/UNESCO-Portugal).

References

[1] N. Hosogai, A. Fukuhara, K. Oshima, Y. Miyata, S. Tanaka, K. Segawa, S. Furukawa, Y. Tochino, R. Komuro, M. Matsuda, I. Shimomura, Adipose tissue hypoxia in obesity and its impact on adipocytokine dysregulation, Diabetes, 56 (2007) 901-911.
[2] M.E. Rausch, S. Weisberg, P. Vardhana, D.V. Tortoriello, Obesity in C57BL/6J mice is characterized by adipose tissue hypoxia and cytotoxic T-cell infiltration, International journal of obesity, 32 (2008) 451-463.
[3] J. Ye, Z. Gao, J. Yin, Q. He, Hypoxia is a potential risk factor for chronic inflammation and adiponectin reduction in adipose tissue of ob/ob and dietary obese mice, American journal of physiology. Endocrinology and metabolism, 293 (2007) E1118-1128.
[4] B. Kabon, A. Nagele, D. Reddy, C. Eagon, J.W. Fleshman, D.I. Sessler, A. Kurz, Obesity decreases perioperative tissue oxygenation, Anesthesiology, 100 (2004) 274-280.
[5] T. Skurk, C. Alberti-Huber, C. Herder, H. Hauner, Relationship between adipocyte size and adipokine expression and secretion, The Journal of clinical endocrinology and metabolism, 92 (2007) 1023-1033.
[6] M.C. Brahimi-Horn, J. Pouyssegur, Oxygen, a source of life and stress, FEBS letters, 581 (2007) 3582-3591.
[7] G.L. Wang, B.H. Jiang, E.A. Rue, G.L. Semenza, Hypoxia-inducible factor 1 is a basic-helix-loop-helix-PAS heterodimer regulated by cellular O2 tension, Proceedings of the National Academy of Sciences of the United States of America, 92 (1995) 5510-5514.
[8] W. Liu, S.M. Shen, X.Y. Zhao, G.Q. Chen, Targeted genes and interacting proteins of hypoxia inducible factor-1, International journal of biochemistry and molecular biology, 3 (2012) 165-178.
[9] E.D. Rosen, O.A. MacDougald, Adipocyte differentiation from the inside out, Nature reviews. Molecular cell biology, 7 (2006) 885-896.
[10] Z. Yun, H.L. Maecker, R.S. Johnson, A.J. Giaccia, Inhibition of PPAR gamma 2 gene expression by the HIF-1-regulated gene DEC1/Stra13: a mechanism for regulation of adipogenesis by hypoxia, Developmental cell, 2 (2002) 331-341.
[11] K.H. Kim, M.J. Song, J. Chung, H. Park, J.B. Kim, Hypoxia inhibits adipocyte differentiation in a HDAC-independent manner, Biochemical and biophysical research communications, 333 (2005) 1178-1184.
[12] T. Fink, L. Abildtrup, K. Fogd, B.M. Abdallah, M. Kassem, P. Ebbesen, V. Zachar, Induction of adipocyte-like phenotype in human

mesenchymal stem cells by hypoxia, Stem cells, 22 (2004) 1346-1355.
[13] Y.S. Park, Y. Huang, Y.J. Park, A.E. David, L. White, H. He, H.S. Chung, V.C. Yang, Specific down regulation of 3T3-L1 adipocyte differentiation by cell-permeable antisense HIF1alpha-oligonucleotide, Journal of controlled release : official journal of the Controlled Release Society, 144 (2010) 82-90.
[14] Q. Lin, Y.J. Lee, Z. Yun, Differentiation arrest by hypoxia, The Journal of biological chemistry, 281 (2006) 30678-30683.
[15] J. Krishnan, C. Danzer, T. Simka, J. Ukropec, K.M. Walter, S. Kumpf, P. Mirtschink, B. Ukropcova, D. Gasperikova, T. Pedrazzini, W. Krek, Dietary obesity-associated Hif1alpha activation in adipocytes restricts fatty acid oxidation and energy expenditure via suppression of the Sirt2-NAD+ system, Genes & development, 26 (2012) 259-270.
[16] S. Vankoningsloo, M. Piens, C. Lecocq, A. Gilson, A. De Pauw, P. Renard, C. Demazy, A. Houbion, M. Raes, T. Arnould, Mitochondrial dysfunction induces triglyceride accumulation in 3T3-L1 cells: role of fatty acid beta-oxidation and glucose, Journal of lipid research, 46 (2005) 1133-1149.
[17] G. Solaini, A. Baracca, G. Lenaz, G. Sgarbi, Hypoxia and mitochondrial oxidative metabolism, Biochimica et biophysica acta, 1797 (2010) 1171-1177.
[18] J. Boren, K.M. Brindle, Apoptosis-induced mitochondrial dysfunction causes cytoplasmic lipid droplet formation, Cell death and differentiation, 19 (2012) 1561-1570.
[19] E.K. Lee, M.J. Lee, K. Abdelmohsen, W. Kim, M.M. Kim, S. Srikantan, J.L. Martindale, E.R. Hutchison, H.H. Kim, B.S. Marasa, R. Selimyan, J.M. Egan, S.R. Smith, S.K. Fried, M. Gorospe, miR-130 suppresses adipogenesis by inhibiting peroxisome proliferator-activated receptor gamma expression, Molecular and cellular biology, 31 (2011) 626-638.
[20] C. Esau, X. Kang, E. Peralta, E. Hanson, E.G. Marcusson, L.V. Ravichandran, Y. Sun, S. Koo, R.J. Perera, R. Jain, N.M. Dean, S.M. Freier, C.F. Bennett, B. Lollo, R. Griffey, MicroRNA-143 regulates adipocyte differentiation, The Journal of biological chemistry, 279 (2004) 52361-52365.
[21] R. Takanabe, K. Ono, Y. Abe, T. Takaya, T. Horie, H. Wada, T. Kita, N. Satoh, A. Shimatsu, K. Hasegawa, Up-regulated expression of microRNA-143 in association with obesity in adipose tissue of mice fed high-fat diet, Biochemical and biophysical research communications, 376 (2008) 728-732.

[22] Q. Lin, Z. Gao, R.M. Alarcon, J. Ye, Z. Yun, A role of miR-27 in the regulation of adipogenesis, The FEBS journal, 276 (2009) 2348-2358.
[23] S.Y. Kim, A.Y. Kim, H.W. Lee, Y.H. Son, G.Y. Lee, J.W. Lee, Y.S. Lee, J.B. Kim, miR-27a is a negative regulator of adipocyte differentiation via suppressing PPARgamma expression, Biochemical and biophysical research communications, 392 (2010) 323-328.
[24] R. Baerga, Y. Zhang, P.H. Chen, S. Goldman, S. Jin, Targeted deletion of autophagy-related 5 (atg5) impairs adipogenesis in a cellular model and in mice, Autophagy, 5 (2009) 1118-1130.
[25] L. Gui, B. Liu, G. Lv, Hypoxia induces autophagy in cardiomyocytes via a hypoxia-inducible factor 1-dependent mechanism, Experimental and therapeutic medicine, 11 (2016) 2233-2239.
[26] G. Bellot, R. Garcia-Medina, P. Gounon, J. Chiche, D. Roux, J. Pouyssegur, N.M. Mazure, Hypoxia-induced autophagy is mediated through hypoxia-inducible factor induction of BNIP3 and BNIP3L via their BH3 domains, Molecular and cellular biology, 29 (2009) 2570-2581.
[27] R. Singh, Y. Xiang, Y. Wang, K. Baikati, A.M. Cuervo, Y.K. Luu, Y. Tang, J.E. Pessin, G.J. Schwartz, M.J. Czaja, Autophagy regulates adipose mass and differentiation in mice, The Journal of clinical investigation, 119 (2009) 3329-3339.
[28] J. Kovsan, M. Bluher, T. Tarnovscki, N. Kloting, B. Kirshtein, L. Madar, I. Shai, R. Golan, I. Harman-Boehm, M.R. Schon, A.S. Greenberg, Z. Elazar, N. Bashan, A. Rudich, Altered autophagy in human adipose tissues in obesity, The Journal of clinical endocrinology and metabolism, 96 (2011) E268-277.
[29] Y. Yuan, G. Hilliard, T. Ferguson, D.E. Millhorn, Cobalt inhibits the interaction between hypoxia-inducible factor-alpha and von Hippel-Lindau protein by direct binding to hypoxia-inducible factor-alpha, The Journal of biological chemistry, 278 (2003) 15911-15916.
[30] M. Hirsila, P. Koivunen, L. Xu, T. Seeley, K.I. Kivirikko, J. Myllyharju, Effect of desferrioxamine and metals on the hydroxylases in the oxygen sensing pathway, FASEB journal : official publication of the Federation of American Societies for Experimental Biology, 19 (2005) 1308-1310.
[31] C.M. Smas, H.S. Sul, Pref-1, a protein containing EGF-like repeats, inhibits adipocyte differentiation, Cell, 73 (1993) 725-734.
[32] J. Boren, K.M. Brindle, Apoptosis-induced mitochondrial dysfunction causes cytoplasmic lipid droplet formation, Cell Death Differ, (2012).

[33] M. Karbiener, C. Fischer, S. Nowitsch, P. Opriessnig, C. Papak, G. Ailhaud, C. Dani, E.Z. Amri, M. Scheideler, microRNA miR-27b impairs human adipocyte differentiation and targets PPARgamma, Biochemical and biophysical research communications, 390 (2009) 247-251.
[34] A. Priyanka, S.S. Anusree, V.M. Nisha, K.G. Raghu, Curcumin improves hypoxia induced dysfunctions in 3T3-L1 adipocytes by protecting mitochondria and down regulating inflammation, BioFactors, 40 (2014) 513-523.
[35] Y. Chen, M.B. Azad, S.B. Gibson, Superoxide is the major reactive oxygen species regulating autophagy, Cell death and differentiation, 16 (2009) 1040-1052.
[36] N. Mizushima, T. Yoshimori, B. Levine, Methods in mammalian autophagy research, Cell, 140 (2010) 313-326.
[37] J. Yin, Z. Gao, Q. He, D. Zhou, Z. Guo, J. Ye, Role of hypoxia in obesity-induced disorders of glucose and lipid metabolism in adipose tissue, American journal of physiology. Endocrinology and metabolism, 296 (2009) E333-342.
[38] T. Hashimoto, T. Yokokawa, Y. Endo, N. Iwanaka, K. Higashida, S. Taguchi, Modest hypoxia significantly reduces triglyceride content and lipid droplet size in 3T3-L1 adipocytes, Biochemical and biophysical research communications, 440 (2013) 43-49.
[39] D. Ren, T.N. Collingwood, E.J. Rebar, A.P. Wolffe, H.S. Camp, PPARgamma knockdown by engineered transcription factors: exogenous PPARgamma2 but not PPARgamma1 reactivates adipogenesis, Genes & development, 16 (2002) 27-32.
[40] H. Ren, Y. Cao, Q. Zhao, J. Li, C. Zhou, L. Liao, M. Jia, Q. Zhao, H. Cai, Z.C. Han, R. Yang, G. Chen, R.C. Zhao, Proliferation and differentiation of bone marrow stromal cells under hypoxic conditions, Biochemical and biophysical research communications, 347 (2006) 12-21.
[41] S. Sano, Y. Izumi, T. Yamaguchi, T. Yamazaki, M. Tanaka, M. Shiota, M. Osada-Oka, Y. Nakamura, M. Wei, H. Wanibuchi, H. Iwao, M. Yoshiyama, Lipid synthesis is promoted by hypoxic adipocyte-derived exosomes in 3T3-L1 cells, Biochemical and biophysical research communications, 445 (2014) 327-333.
[42] S.Z. Chen, X. Xu, L.F. Ning, W.Y. Jiang, C. Xing, Q.Q. Tang, H.Y. Huang, miR-27 impairs the adipogenic lineage commitment via targeting lysyl oxidase, Obesity, 23 (2015) 2445-2453.
[43] S. Vankoningsloo, A. De Pauw, A. Houbion, S. Tejerina, C. Demazy, F. de Longueville, V. Bertholet, P. Renard, J. Remacle, P. Holvoet, M. Raes, T. Arnould, CREB activation induced by

mitochondrial dysfunction triggers triglyceride accumulation in 3T3-L1 preadipocytes, Journal of cell science, 119 (2006) 1266-1282.
[44] W. Wang, Y. Zhang, W. Lu, K. Liu, Mitochondrial reactive oxygen species regulate adipocyte differentiation of mesenchymal stem cells in hematopoietic stress induced by arabinosylcytosine, PloS one, 10 (2015) e0120629.
[45] H. Lee, Y.J. Lee, H. Choi, E.H. Ko, J.W. Kim, Reactive oxygen species facilitate adipocyte differentiation by accelerating mitotic clonal expansion, The Journal of biological chemistry, 284 (2009) 10601-10609.
[46] Y. Lin, A.H. Berg, P. Iyengar, T.K. Lam, A. Giacca, T.P. Combs, M.W. Rajala, X. Du, B. Rollman, W. Li, M. Hawkins, N. Barzilai, C.J. Rhodes, I.G. Fantus, M. Brownlee, P.E. Scherer, The hyperglycemia-induced inflammatory response in adipocytes: the role of reactive oxygen species, The Journal of biological chemistry, 280 (2005) 4617-4626.
[47] I. Talior, T. Tennenbaum, T. Kuroki, H. Eldar-Finkelman, PKC-delta-dependent activation of oxidative stress in adipocytes of obese and insulin-resistant mice: role for NADPH oxidase, American journal of physiology. Endocrinology and metabolism, 288 (2005) E405-411.
[48] Y. Zhang, S. Goldman, R. Baerga, Y. Zhao, M. Komatsu, S. Jin, Adipose-specific deletion of autophagy-related gene 7 (atg7) in mice reveals a role in adipogenesis, Proceedings of the National Academy of Sciences of the United States of America, 106 (2009) 19860-19865.

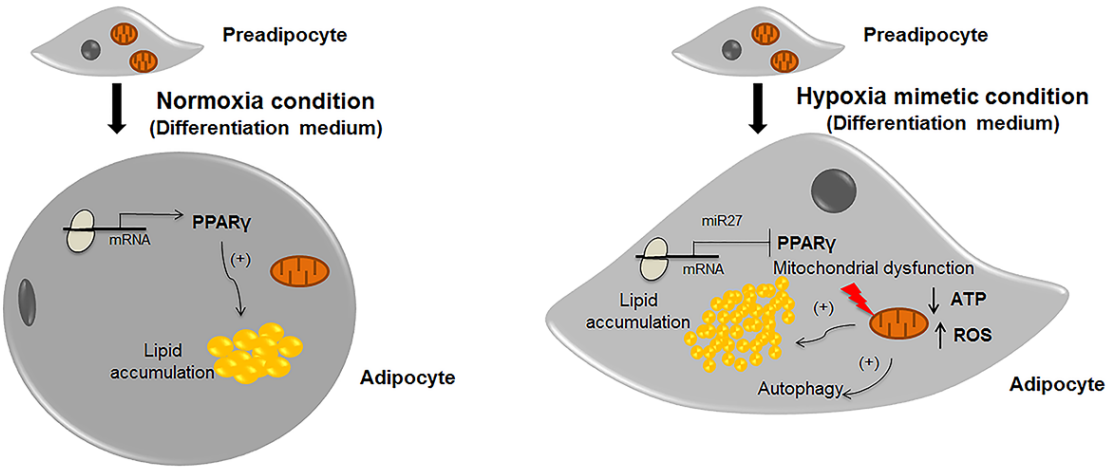

Graphical abstract

Highlights:

- Hypoxia mimetic inhibits adipocyte differentiation and increases miR-27a and b.
- Hypoxia mimetic causes mitochondrial dysfunction and an increase in reactive oxygen species.
- Hypoxia mimetic induces lipid accumulation through reactive oxygen species increase.
- Hypoxia mimetic induces autophagy activation.